J Membrane Biol (2008) 222:91–106
DOI 10.1007/s00232-008-9105-9

Mutations at Arginine 352 Alter the Pore Architecture of CFTR

Guiying Cui · Zhi-Ren Zhang · Andrew R. W. O'Brien · Binlin Song · Nael A. McCarty

Received: 29 August 2007 / Accepted: 21 March 2008 / Published online: 18 April 2008

Abstract Arginine 352 (R352) in the sixth transmembrane domain of the cystic fibrosis transmembrane conductance regulator (CFTR) previously was reported to form an anion/cation selectivity filter and to provide positive charge in the intracellular vestibule. However, mutations at this site have nonspecific effects, such as inducing susceptibility of endogenous cysteines to chemical modification. We hypothesized that R352 stabilizes channel structure and that charge-destroying mutations at this site disrupt pore architecture, with multiple consequences. We tested the effects of mutations at R352 on conductance, anion selectivity and block by the sulfonylurea drug glipizide, using recordings of wild-type and mutant channels. Charge-altering mutations at R352 destabilized the open state and altered both selectivity and block. In contrast, R352K-CFTR was similar to wild-type. Full conductance state amplitude was similar to that of wild-type CFTR in all mutants except R352E, suggesting that R352 does not itself form an anion coordination site. In an attempt to identify an acidic residue that may interact with R352, we found that permeation properties were similarly affected by charge-reversing mutations at D993. Wild-type-like properties were rescued in R352E/D993R-CFTR, suggesting that R352 and D993 in the wild-type channel may interact to stabilize pore architecture. Finally, R352A-CFTR was sensitive to modification by externally applied $MTSEA^+$, while wild-type and R352E/D993R-CFTR were not. These data suggest that R352 plays an important structural role in CFTR, perhaps reflecting its involvement in forming a salt bridge with residue D993.

Keywords CFTR · Chloride channel · Salt bridge · Channel open state · Subconductance · Blocker · Anion selectivity

G. Cui · Z.-R. Zhang · A. R. W. O'Brien · B. Song · N. A. McCarty
School of Biology, Georgia Institute of Technology, Atlanta, GA 30332-0230, USA

G. Cui
e-mail: gcui2@emory.edu

N. A. McCarty (✉) · G. Cui
Division of Pulmonology, Allergy/Immunology, Cystic Fibrosis, and Sleep, Department of Pediatrics, Emory University School of Medicine, 2015 Uppergate Drive, Atlanta, GA 30322, USA
e-mail: namccar@emory.edu

Introduction

The cystic fibrosis transmembrane conductance regulator (CFTR) forms a chloride channel whose gating is regulated by phosphorylation by protein kinase A (PKA) plus binding and hydrolysis of ATP (Riordan et al. 1989; Cheng et al. 1990, 1991; Anderson et al. 1991; Baukrowitz et al. 1994; Hwang et al. 1994; Gadsby et al. 2006; Guggino and Stanton 2006); CFTR is a member of the large ATP binding cassette (ABC) transporter superfamily (Dean et al. 2001). The proposed overall structure of CFTR consists of five functional domains: two hydrophobic membrane-spanning domains (MSD1, MSD2), each including six transmembrane (TM) helices; two hydrophilic membrane-associated domains, containing sequences that form nucleotide-binding domains (NBD1, NBD2); and a regulatory (R) domain (Riordan et al. 1989; Devidas and Guggino 1997).

The majority of the work investigating the CFTR pore has focused on TM6, including residues 334–353 (McCarty 2000; Linsdell 2006). For example, R334 and K335 are located in the outer vestibule of the CFTR pore and influence selectivity and Cl^- conductance (Smith et al. 2001; McCarty and Zhang

2001; Zhang et al. 2005a, b). T338 and T339 together control the permeability of the channel to polyatomic anions as if they contribute to a narrow region in the pore (McDonough et al. 1994; Linsdell et al. 1997; McCarty and Zhang 2001; Liu et al. 2004). S341 lies at the cytoplasmic end of the narrow region and contributes to anion selectivity, single-channel conductance and the binding site for some pore blockers (McDonough et al. 1994; McCarty and Zhang 2001). R347, near the predicted cytoplasmic end of the pore, has been the focus of several investigations. Tabcharani et al. (1993) showed that anomalous mole-fraction behavior in mixtures of SCN^- and Cl^- was lost in R347D-CFTR and that this mutation also reduced single-channel conductance. Other investigators proposed that R347 functions in anion selectivity and block by cytoplasmic 4,4′-diisothiocyanatostilbene-2,2′-disulfonic acid (DIDS) (Linsdell and Hanrahan 1996a, b; Cheung and Akabas 1997; Tabcharani et al. 1997). Alternatively, Cotten and Welsh (1999) reported that R347 plays an important role in regulating the overall structure of the CFTR pore; R347P-CFTR exhibited significantly decreased single-channel conductance and unstable channel openings, while R347H-CFTR displayed a pH-dependent conductance and anomalous mole-fraction behavior. In contrast, R347K-CFTR exhibited permeation properties similar to those of wild-type (WT)-CFTR. This suggested that substitutions at R347 to amino acids other than lysine disrupted an important structural feature of the pore, perhaps causing gross changes in pore structure that lead to anomalous function and instability of the open state. The D924R mutation in TM8 complemented the R347D mutation, reverting the channel to WT behavior, allowing the authors to conclude that R347 functions at least in part by forming a salt bridge with D924 (Cotten and Welsh 1999).

Residues in TM domains other than TM6 have been investigated as well (Sheppard et al. 1996; McCarty 2000; Ge et al. 2004; Linsdell 2005). Dawson and coworkers have suggested that TM5 may contribute to the pore based on the finding that mutations at G314 and V317 alter conduction properties (Zhang et al. 2001; Smith et al. 2001). By contrast, Ge et al. (2004) suggested that TMs 1 and 6 make the strongest contributions to defining the permeation properties of open CFTR channels; other TM domains, including TM12 (McDonough et al. 1994; Ge et al. 2004) likely also contribute to the pore. The assembled structure of these TM domains in the WT channel is finely tuned to provide stable channel openings with consistent permeation properties.

R352 is predicted to lie near the cytoplasmic end of TM6. Three cystic fibrosis (CF)–associated mutations have been identified at this position (R352G, R352W and R352Q), but the mechanisms by which these mutations cause disease are not clear (Cremonesi et al. 1992; Audrézet et al. 1993; Brancolini et al. 1995). It was suggested previously that T351, R352 and Q353 formed a reentrant loop that established the anion/cation selectivity filter of CFTR based on Cl^- to Na^+ permeability ratios and the rates of reaction to positively and negatively charged methanethiosulfonate (MTS) reagents of cysteines engineered at this site, with R352 acting as a major determinant of charge selectivity (Cheung and Akabas 1997; Guinamard and Akabas 1999; St. Aubin and Linsdell 2006). However, mutations at R352 also have consequences that cannot be attributed to simple loss of positive charge (e.g., Smith et al. 2001). To better understand the role of R352 in CFTR structure and function, we examined the effects on permeation properties of mutations at R352, as well as at various acidic residues in other TM helices that might interact with R352. The data suggest that R352 does not play a direct role in selectivity and conductance in CFTR but helps to maintain the gross architecture of the channel pore, thereby indirectly controlling permeation properties.

Methods

Preparation of Oocytes and cRNA

The mutants used in this study were prepared using site-directed mutagenesis with the Quikchange protocol (Stratagene, La Jolla, CA). All cRNAs except WT-CFTR for single-channel recording were prepared from constructs encoding CFTR in the pGEMHE vector, which was kindly provided by Dr. D. Gadsby (Rockefeller University, New York, NY). WT-CFTR cRNA for single-channel recording was prepared from a construct in the pAlter vector (Promega, Madison, WI). All mutant constructs were verified by sequencing across the entire open reading frame before use. *Xenopus laevis* oocytes were injected in a range of 10–100 ng of CFTR cRNAs and incubated at 18 °C in modified Liebovitz's L-15 medium with the addition of HEPES (pH 7.5), gentamicin and penicillin/streptomycin. Recordings were made 24–72 h after the injection of cRNAs. Methods of animal handling were in accordance with National Institutes of Health guidelines, and the protocol was approved by the Animal Use and Care Committee of the Georgia Institute of Technology.

Electrophysiology

For single-channel recording, CFTR channels were studied in excised, inside–out patches at room temperature (22–23 °C). Oocytes were prepared for study by shrinking in hypertonic solution (in mM: 200 monopotassium aspartate, 20 KCl, 1 $MgCl_2$, 10 EGTA and 10 HEPES-KOH, pH 7.2), followed by manual removal of the vitelline membrane. Pipettes were pulled from borosilicate glass (Sutter

Instrument, Novato, CA) and had resistances averaging ~10 MΩ when filled with chloride-containing pipette solution (in mM: 150 NMDG-Cl, 5 $MgCl_2$ and 10 TES, pH 7.5). Typical seal resistances were 200 GΩ or greater. Channels were activated by excision into intracellular solution (in mM: 150 NMDG-Cl, 1.1 $MgCl_2$, 2 Tris-EGTA, 10 TES, 1 MgATP and 50 U/mL PKA, pH 7.5). CFTR currents were measured with an Axopatch 200B amplifier (Axon Instruments, Union City, CA) and recorded at 10 kHz to DAT tape. For subsequent analysis, records were played back and filtered with a four-pole Bessel filter (Warner Instruments, Hamden, CT) at a corner frequency of 100 Hz and acquired using a Digidata 1322A interface (Axon Instruments) and computer at 500 Hz with pClamp 8.2 software (Axon Instruments). For display, single-channel records were filtered digitally to 70 Hz.

For inside–out macropatch recording, electrodes were filled with the same solution as for single-channel recording, with resistances averaging ~1–2 MΩ. Typical seal resistances were 100 GΩ or greater. Macropatch recordings also were performed with an Axopatch 200B amplifier operated with pClamp 8.2; data were filtered at 100 Hz and acquired at ≥2 kHz. The normal intracellular control solution contained (in mM) 150 NaCl, 1.1 $MgCl_2$, 2 Tris-EGTA, 10 TES and 1 MgATP (pH 7.45). Channels were activated by exposure to 50 U/ml PKA (Promega). For selectivity experiments, the substitution solutions contained (in mM) 130 Na salt (NaSCN, $NaNO_3$ or NaBr), 20 NaCl, 1.1 $MgCl_2$, 2 Tris-EGTA, 10 TES and 1 MgATP (pH 7.45). Data were corrected for junction potentials at the ground bridge (3 M KCl in 4% agar), which ranged 0.5–9.1 mV as determined with a free-flowing KCl electrode (McCarty and Zhang 2001). Substitutions were always made in the same order and for a 1-min duration before recording. CFTR macropatch currents for selectivity experiments were generated with a depolarizing ramp protocol, holding at $V_M = -100$ mV for 60 ms, followed by a ramp to +100 mV over the course of 200 ms (as shown later, in Fig. 5). The protocol was run in triplicate, and the data were averaged. For experiments with pore blockers, we used the same solution as for single-channel recording but added glipizide to a final concentration of 200 μM. We used two protocols for experiments with blockers. One used a holding potential of 0 mV, followed by a step to +80 mV for 150 ms, then to −120 mV for 150 ms, then to +100 mV for 150 ms before returning to 0 mV (as shown later, in Fig. 6A, C, E, G). Another protocol used a holding potential of −100 mV, followed by a ramp between −100 and +100 mV over 200 ms (as shown later, in Fig. 6B, D, F, H). The protocol was run three times, and the averaged data were used for analysis and display. In all cases, blocker was applied using a fast-perfusion system (Warner Instruments, model SF–77B).

Oocytes expressing CFTR and the β_2-adrenergic receptor were studied by two-electrode voltage clamp (GeneClamp 500 amplifier, Axon Instruments) in order to determine the consequences of exposure to the membrane-permeant sulfhydryl-modifying reagent methanethiosulfonate ethylammonium ($MTSEA^+$). Oocytes were incubated for 20 min in ND96 solution (in mM: 96 NaCl, 2 KCl, 1 $MgCl_2$ and 5 HEPES, pH 7.5) containing 2 mM dithiothreitol (DTT), to set the redox status of accessible cysteine residues, in order to normalize the potential responses to subsequent exposure to $MTSEA^+$ (Liu et al. 2004). CFTR currents were activated by exposure to 1 μM isoproterenol. Once channel activation reached plateau, cells were exposed to ND96 containing 1 mM $MTSEA^+$ in the continuous presence of isoproterenol. For analysis, currents after 5-min exposure to $MTSEA^+$ were compared to plateau currents before $MTSEA^+$.

Analysis of Single-Channel and Macropatch Experiments

pClamp version 9.0 was used to make all-points amplitude histograms, which had bin widths of 0.01 pA and were fit with gaussian distributions using Clampfit. Open and closed current levels were first identified manually, and then transition analysis using a 50% cut-off between open and closed levels was employed. Channels formed by R352A, Q and E mutants and some double mutants exhibited multiple conductance levels, with *s1* representing subconductance level 1; *s2*, subconductance level 2; *f*, full conductance level; and *c*, closed conductance level, as previously described (Zhang et al. 2005a, b). Single-channel slope conductances were determined by linear regression.

To determine how mutations at R352 affected the stability of the open state, single-channel records from WT-CFTR and R352A-CFTR were analyzed using Clampfit and QuB (http://www.qub.buffalo.edu) (Qin et al. 2006). After filtering data files at 50 Hz, sections with baseline noise that would obscure transitions or with concurrent openings of multiple channels were set to zero, from the end of the last clean burst to the end of the last unusable burst, in order to avoid contamination of the analysis. Data files were then opened in QuB, where the zeroed portions were removed. QuB was then used to idealize the record using a five-state model consisting of the following kinetic states representing specific conductance levels of varying durations: *f* conductance, full, maximal single-channel conductance; *s2* subconductance, 70% of full conductance; *s1* subconductance (40% of full conductance); *IC*, intra-burst closed (closed states lasting <100 ms); and *c*, long-lived closed states. Only transitions that were stable for more than 10 ms were counted. QuB calculated the fraction

of time spent in each of the five states over the course of the record.

For macropatch blocker experiments, we calculated the fractional block at $V_M = -120$ mV, after current reached steady state, according to the equation

$$\text{Fractional block} = 1 - (I_b/I) \quad (1)$$

where I_b is the steady-state current in the presence of blocker and I is the steady-state current before blocker.

For macropatch selectivity experiments, patches were exposed to solution containing substitute anions bracketed by measurements in solution containing chloride as the predominant anion (McCarty and Zhang 2001). Relative permeability (P_x/P_{Cl}) and relative conductance (G_x/G_{Cl}) for each substitute anion (anion x) were calculated with the average data for the preceding and subsequent exposures to chloride. This procedure allowed us to compare the G_x/G_{Cl} values for several anions by controlling for the changes in activation during the experiment (McCarty and Zhang 2001). Reversal potentials for Cl^- (V_{rev}^{Cl}) and for each test anion (V_{rev}^{x}) were used to calculate P_x/P_{Cl} values according to the Goldman-Hodgkin-Katz equation in the following form:

$$P_x/P_{Cl} = \left\{[Cl]_r 10^{zF\Delta Vr/RT} - [Cl^-]_t\right\} \Big/ [x^-]_t \quad (2)$$

where $[Cl^-]_r$ and $[Cl^-]_t$ are the concentrations of chloride in the reference and test solutions, respectively; $[x^-]_t$ is the concentration of anion x in the test solution (130 mM); ΔVr is the change in V_{rev}; z is the valence; R is the gas constant; T is the absolute temperature; and F is the Faraday constant (McCarty and Zhang 2001). Relative chord conductances for exit of intracellular anions were calculated from the change in current over a voltage range from $V_M = V_{rev}$ to $V_M = V_{rev} - 25$ mV. All macropatch data were background-subtracted, using as background the current measured before activation of CFTR by PKA and ATP.

Source of Reagents

Unless otherwise noted, all reagents were obtained from Sigma (St. Louis, MO). L-15 medium was from GIBCO/BRL (Gaithersburg, MD). NaBr and NaSCN were from Baker (Phillipsburg, NJ). $NaNO_3$ was from Fisher Scientific (Fair Lawn, NJ). PKA was from Promega. Glipizide was prepared as a stock solution in dimethyl sulfoxide (DMSO) at 0.1 M and diluted to 200 μM final concentration immediately before use. At the concentration used, DMSO was without effect on CFTR currents (data not shown).

Statistics

Unless otherwise noted, values are means ± SEM. Statistical analysis was performed using the t-test for unpaired or paired measurements by Sigma Stat 2.03 (Jandel Scientific, San Rafael, CA), with $P < 0.05$ considered indicative of significance.

Results

Charge-Neutralizing Substitutions at R352 Affect the Stability of the Open State

R347 and R352 are two basic residues in the CFTR TM6. Previous studies showed that both R347C and R352C either were not accessible to membrane-impermeant MTS reagents (methanethiosulfonate ethyltrimethylammonium [$MTSET^+$] or methanethiosulfonate ethylsulfonate [$MTSES^-$]) applied to the extracellular solution or lacked significant functional consequences when modified; this suggested that both sites either were at the predicted cytoplasmic end of the pore, and therefore cytoplasmic to the narrow region, or were not pore-facing residues (Smith et al. 2001). R352C was, however, sensitive to membrane-permeant $MTSEA^+$. Surprisingly, mutation R352Q also resulted in sensitivity to $MTSEA^+$, suggesting that loss of positive charge at position 352 caused an endogenous cysteine to become available for modification, perhaps reflecting loss of gross pore structure. Previously, it was reported that loss of positive charge at position 347 had a similar pleiotropic effect on altering pore geometry due to its role in forming a salt bridge with D924 in TM8 (Cotten and Welsh 1999). It seemed possible that R352 may serve a similar role in preserving the architecture of the channel pore.

If R347 and R352 function to preserve gross pore architecture, then loss of these residues would be expected to destabilize channel openings. WT-CFTR opens principally to the full conductance state (f, ~7.6 pS at 150 mM $[Cl^-]$) with infrequent transitions to two subconductance states, which we label *s1* (~3.1 pS) and *s2* (~5.4 pS); other very brief conducting states may also exist (Zhang et al. 2005a). We showed previously that these transitions between open conductance states reflect the behavior of a single pore in CFTR, perhaps due to conformational changes in the pore domain coupled to ATP-dependent channel gating (Zhang et al. 2005a, b). Transitions to these subconductance levels occur rarely in WT-CFTR but more frequently in some pore-domain mutants, such as R334C and T338A, although the relative conductances between levels *s1*, *s2*, and *f* are maintained (Zhang et al. 2005a). Hence, the appearance of subconductance states is not necessarily caused by these mutations, although the stability of the subconductance states relative to the full conductance state can be altered in pore-domain mutants (Zhang et al. 2005a).

If mutations at R352 disrupted the pore architecture of CFTR, we expected that the single-channel conductance

would show random occupancy of these conducting states compared to recordings of WT-CFTR. To determine whether R352 mutant channels exhibit instability of the open conductance states, we studied single channels in excised inside–out patches. Figure 1 (left) shows representative single-channel traces of WT-CFTR and selected R352 mutants. Figure 1 (right) shows the all-points amplitude histograms for each trace shown at the left. Both R352A- and R352Q-CFTR showed three distinct open conductance states: *s1*, *s2* and *f*. In contrast to WT-CFTR, channels formed by R352A- and R352Q-CFTR occupied the *s1* and *s2* states in the vast majority of open bursts, while transitions to the *f* conductance state were rare events. These data suggest that the pore architecture of CFTR was altered in these mutants such that the open state was made unstable. The transitions between the three open states in R352A- and R352Q-CFTR were random, showing no regular pattern. In contrast, our previous experiments (Zhang et al. 2005a) with R334C-CFTR showed a more regular transition pattern: Within nearly every burst there were transitions to all three conductance states, with most bursts ending in the *f* state.

To ensure that the multilevel openings presented in Fig. 1 did not simply reflect the concurrent and summed activity of multiple individual channels, each with full conductance significantly lower than that of WT-CFTR, we recorded channel behavior in patches with low activity. A representative recording is shown in Fig. 2. In this patch, six openings from the closed conductance level are evident; the lower traces, at higher temporal resolution, show that these openings exhibited instability of the open state. Importantly, no isolated openings with conductance equivalent to that of either subconductance level were observed as transitions from the closed current level in this record, suggesting that all openings to the full-conductance level in this record represented the activity of a single-channel pore. These results suggest that the designated full conductance level we report here, which is larger than that reported by St. Aubin and Linsdell (2006) for the same mutations, is not an artifact arising from the near simultaneous opening of two lower-conductance channels in records with high activity such as those shown in Fig. 1.

R352K-CFTR showed single-channel properties very similar to those of WT-CFTR: Transitions to the *s1* and *s2* conductance states were rare events in this mutant (Fig. 1D). It seems likely that the R-to-K mutation preserved the positive charge and maintained the pore architecture similar to that of WT-CFTR. This result suggests that a large positively charged residue (arginine or lysine) at position 352 in CFTR stabilizes the *f* state relative to the *s1* and *s2* states.

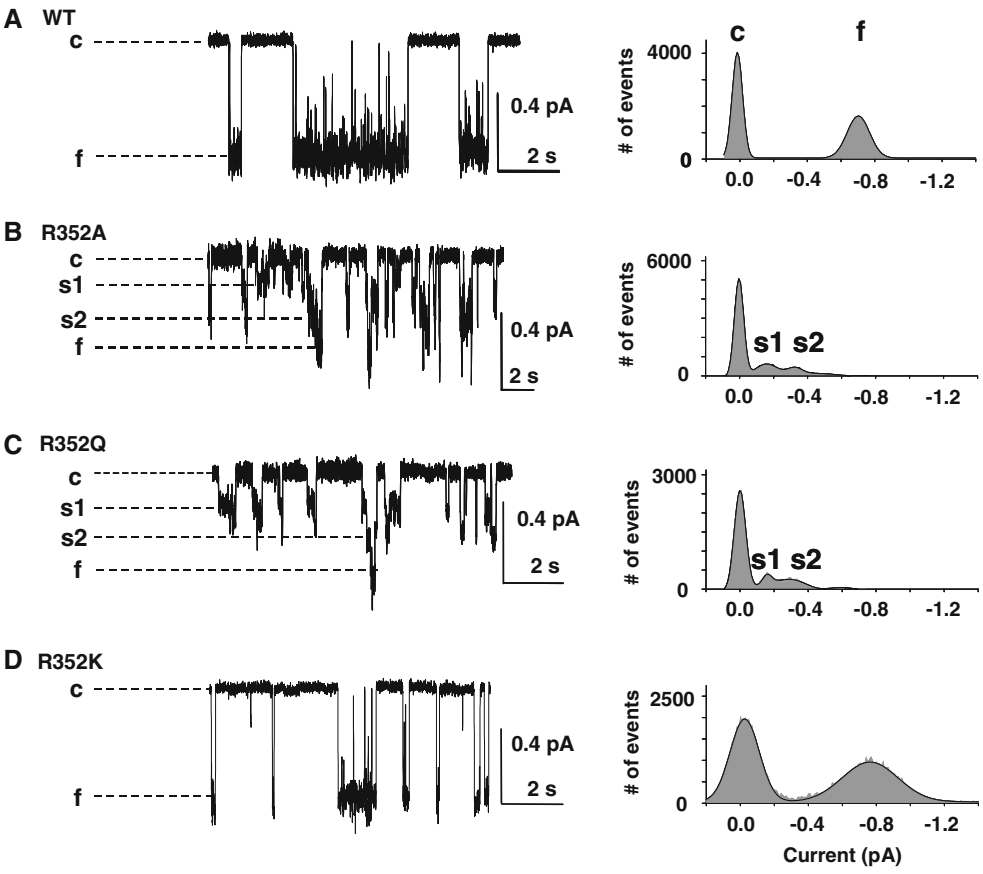

Fig. 1 Sample traces of WT-CFTR and indicated R352 mutants from excised inside–out membrane patches with symmetrical 150 mM Cl^- solution (*left*) and their all-points amplitude histograms (*right*). Each current level is indicated by a *dashed line*. In R352A- and R352Q-CFTR, there are four current levels indicating the *c, s1, s2* and *f* states. All traces were recorded at $V_M = -100$ mV. *Solid lines* in histograms are fit results to the gaussian function in Clampfit 9.0

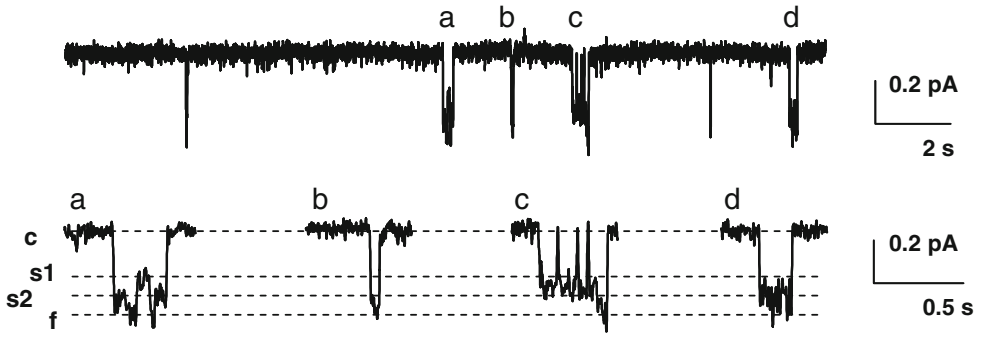

Fig. 2 Instability of open channel current does not reflect summed activity of multiple lower-conductance openings. Shown in the *top trace* is a single record for R352Q-CFTR in a patch with low open probability, $V_M = -80$ mV. Four individual openings are identified (*a–d*). In the lower part of the figure, these four openings are displayed at higher temporal resolution; these openings exhibit conductance transitions between open levels that are not found as transitions from the closed current level

To quantify the effect of mutations at R352 on the stability of the open state, we analyzed intraburst kinetics by determining the fraction of time that each channel spent in the *s1, s2, f* and *IC* states for WT-CFTR and R352A-CFTR. As shown in Fig. 3, WT-CFTR channels spent 96.7 ± 1.3% of each open burst in the *f* state, while R352A-CFTR channels spent only 65.5 ± 17.5% of each burst in the *f* state ($P < 0.02$, mean ± SD for $n = 3$–4 records each). Consistent with previous results, R352A-CFTR channels spent a significantly larger fractional duration of each open burst in the *s1* and *s2* states than did WT-CFTR ($P < 0.001$). We point out that while the data shown in the histograms of Fig. 1 reflect only the records displayed there, with a low number of bursts selected to emphasize transitions to subconductance states, the intraburst kinetic analysis presented here represents 870 s of recording for WT-CFTR, including 510 bursts, and 356 s of recording for R352A-CFTR, including 150 bursts. Interestingly, loss of positive charge at position 352 did not affect the fractional contribution of the *IC* state, suggesting that transitions to this state may reflect conformational changes not limited to the pore domain. Dwell-time analysis of the same records indicated that the mean duration for the *f* state decreased from 632 ± 264 ms in WT-CFTR to 123 ± 63 ms in R352A-CFTR (mean ± SD), representing an 80% reduction in the stability of the fully open state ($n = 3$–4, $P = 0.02$).

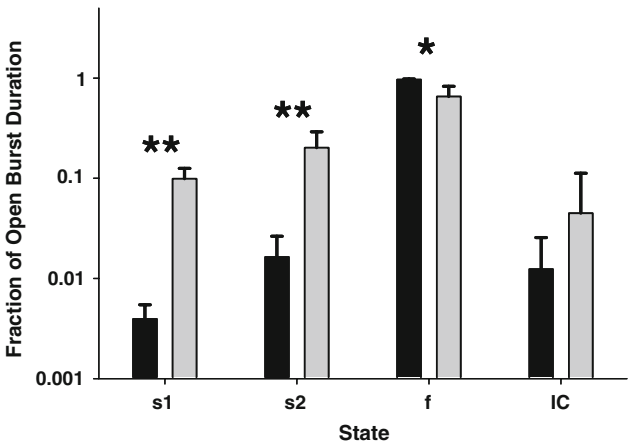

Fig. 3 Stability of the open state and intraburst closed state of WT-CFTR and R352A-CFTR. Mean fraction of open burst duration is plotted for each state of two CFTR constructs (*black bars*, WT-CFTR; *gray bars*, R352A-CFTR). $^{**}P < 0.001$, $^{*}P < 0.02$

To determine whether the residue at position 352 affected absolute single-channel conductance, we examined the *i–V* relationships and slope conductances of the mutant channels. Substate behavior was observed in R352A-CFTR at all voltages (Fig. 4A), including both negative and positive membrane potentials. Figure 4 shows the *i–V* relationship for the *f* conductance states of WT-, R352A-, R352Q- and R352K-CFTR (Fig. 4B) and for the subconductance states of R352A- and R352Q-CFTR (Fig. 4C), at potentials ranging between $V_M = -100$ and +100 mV. The *f* state slope conductance of R352A-CFTR at negative membrane potentials was not different from that of WT-CFTR, suggesting that the positive charge at R352 does not determine channel conductance; at positive membrane potentials, the slope conductance of the *f* state was larger in R352A-CFTR than in WT-CFTR (Table 1). The *f* state slope conductance in R352Q-CFTR was slightly reduced at both negative and positive membrane potentials. Both *f* state slope conductances were significantly reduced in R352E-CFTR (Table 1). In contrast, the slope conductances of R352K-CFTR were very similar to those of WT-CFTR (Table 1). The single-channel conductance of the *f* state exhibited significant outward rectification in R352A-, R352Q- and R352E-CFTR (Table 1). In sum, these results are not consistent with a simple role of R352 in providing positive charge to the intracellular vestibule; if this scenario were true, loss of the positive charge in R352A would be expected to reduce single-channel conductance at both positive and negative potentials but more drastically at

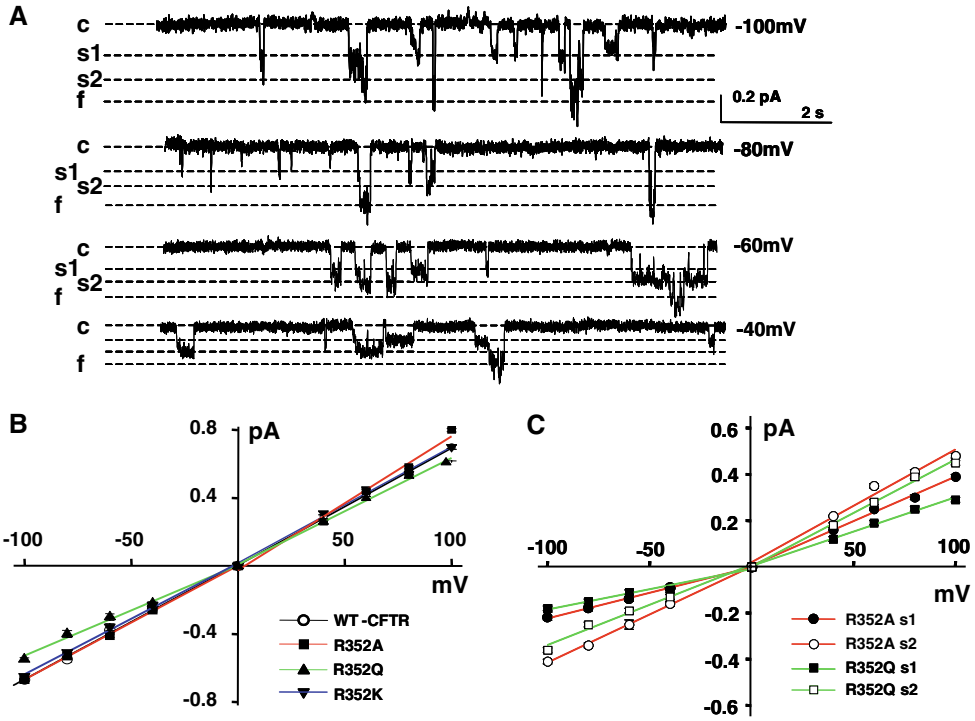

Fig. 4 Sample traces of R352A-CFTR and *i–V* relationships of the conducting states of WT-CFTR and R352 mutants. (**A**) Four traces of R352A-CFTR from a single patch at tested voltages indicated at the *right*. Current levels are indicated by a *dashed line*. (**B**) Single-channel *i–V* relationships for *f* conductance states of R352A-, R352Q- and R352K-CFTR, with WT-CFTR for comparison. Points show mean ± SEM for $n = 5$–7 observations, and error bars are smaller than the symbols; *lines* are from linear regression. (**C**) The *i–V* relationship of the *s1* and *s2* subconductance states of R352A- and R352Q-CFTR. Slope conductances are summarized in Table 1

Table 1 Slope conductance[a] (in pS) of the *f* state of WT-CFTR and multiple single and double mutants

CFTR	*n*	Negative V_M	Positive V_M
WT	7	6.82 ± 0.03	6.97 ± 0.06
R352A	6	6.80 ± 0.06	7.85 ± 0.07*,**
R352Q	6	5.29 ± 0.02*	6.28 ± 0.05*,**
R352K	5	6.87 ± 0.03	6.86 ± 0.01
R352E	5	3.78 ± 0.01*	6.03 ± 0.01*,**
R352E/E873R	6	3.84 ± 0.01*	5.64 ± 0.01*,**
R352E/E1104R	6	4.36 ± 0.01*	5.86 ± 0.02*,**
R352E/D993R	5	5.90 ± 0.02*	6.44 ± 0.01*,**
D993R	7	8.27 ± 0.05*	7.13 ± 0.07**

[a] Slope conductance indicates single-channel conductance calculated from 0 to +100 mV (positive V_M) or to −100 mV (negative V_M) by linear regression

* $P \leq 0.001$ compared to the equivalent slope conductance in WT-CFTR, ** $P \leq 0.001$ compared to the slope conductance in the same mutant at negative V_M

negative membrane potentials, where the local surface charge in the intracellular vestibule would most strongly affect exit of cytoplasmic anions through the channel pore.

Anion Selectivity of R352A-, R352E- and R352K-CFTR

To determine whether mutations at R352 affected the ability of CFTR channels to select between ions of similar charge, we studied the anion selectivity patterns of R352A-, R352E- and R352K-CFTR using inside–out macropatches and compared them to WT-CFTR. Figure 5 shows five representative experiments in cytoplasmic solutions containing 150 mM Cl^- as the predominant anion or solutions containing 20 mM Cl^- and 130 mM substitute anion. We calculated relative permeability (P_x/P_{Cl}) and relative conductance (G_x/G_{Cl}) for WT-CFTR and each mutant (Tables 2, 3). Anions are listed in the tables in the order of their use in experiments, with each substitute anion bracketed by measurements in chloride. All CFTR variants tested displayed the same anion permeability sequence: $SCN^- > NO_3^- \geq Br^- > Cl^-$. These results suggested that mutations at R352 did not alter lyotropic permselectivity (Tabcharani et al. 1997; Smith et al. 1999), although small changes in magnitude were evident in comparison to WT-CFTR. For calculation of G_x/G_{Cl}, we compared R352A-, R352E- and R352K-CFTR with WT-CFTR as well as R352E- and R352K-CFTR with R352A-CFTR. All tested R352 single mutants exhibited significantly increased relative conductance for SCN^-, Br^- and NO_3^- compared to that of WT-CFTR. These data suggested that mutations at position 352 caused a change in the conductance of these small anions but not their permeability. The relative conductance for SCN^- was particularly affected; SCN^- has previously been used as a permeant probe of the CFTR channel pore due to its high sensitivity to alterations of putative anion binding sites (Zhang et al. 2000; Linsdell et al. 2000; Linsdell 2001, 2005). The normalization of relative conductances between the different anions tested likely

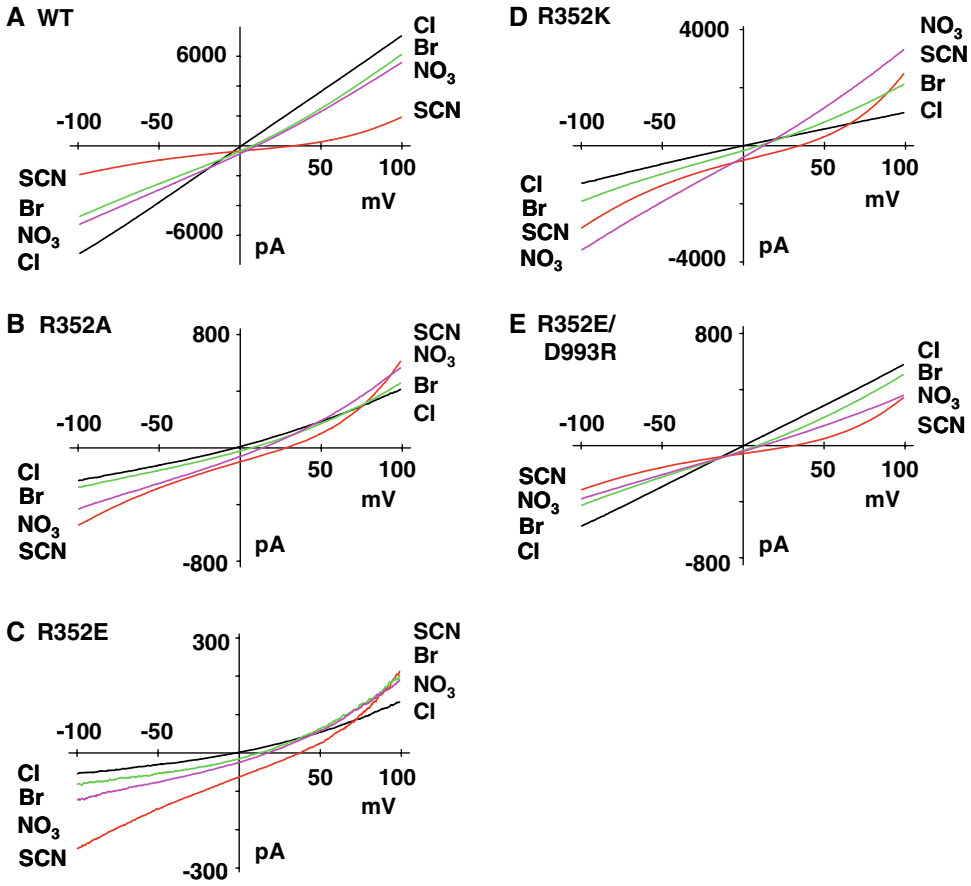

Fig. 5 Mutations at R352 alter anion selectivity. Representative inside–out macropatches, recorded in the presence of cytoplasmic Cl^- or Cl^- plus substitute anions, with voltage ramps between −100 and +100 mV, are shown for (**A**) WT-CFTR, (**B**) R352A-CFTR, (**C**) R352E-CFTR, (**D**) R352K-CFTR and (**E**) the double mutant R352E/D993R-CFTR. Raw currents are shown with background currents subtracted and before correction for junction potentials (see "Methods"). Pipette solution contained 150 mM NMDG-Cl. All data in a given panel come from a single patch. Solutions were at pH 7.45 and are labeled as follows: 150 mM Cl^- (black), 130 mM Cl^- plus 20 mM NO_3^- (purple), 130 mM Cl^- plus 20 mM Br^- (green) and 130 mM Cl^- plus 20 mM SCN^- (red)

Table 2 Relative permeabilities of some anions in WT-CFTR and R352-CFTR mutants

CFTR	*n*	SCN	Br	NO_3
WT	6	4.11 ± 0.17	1.45 ± 0.04	1.51 ± 0.02
R352A	10	4.18 ± 0.65	1.35 ± 0.21	1.70 ± 0.29
R352E	6	5.18 ± 0.32*	1.47 ± 0.08	1.64 ± 0.43
R352K	7	4.05 ± 0.12	1.52 ± 0.01	1.59 ± 0.03**
R352E/D993R	6	3.62 ± 0.06*	1.48 ± 0.04	1.59 ± 0.02**

* Significant difference compared with WT-CFTR, $P < 0.05$; ** Significant difference compared with R352A, $P < 0.05$

Table 3 Relative conductances of some anions in WT-CFTR and R352-CFTR mutants

CFTR	*n*	SCN	Br	NO_3
WT	6	0.16 ± 0.02	0.67 ± 0.04	0.84 ± 0.04
R352A	10	1.59 ± 0.12*	1.31 ± 0.08*	1.59 ± 0.14*
R352E	6	2.73 ± 0.31*·**	1.49 ± 0.22*	1.54 ± 0.12*
R352K	7	1.12 ± 0.08*·**	0.99 ± 0.02*·**	1.73 ± 0.26*
R352E/D993R	7	0.61 ± 0.05*·**	0.98 ± 0.03*·**	1.26 ± 0.13*

Relative conductance was measured at $V_M = V_{rev} - 25$ mV

* Significant difference compared with WT-CFTR, $P < 0.05$; ** Significant difference compared with R352A, $P < 0.05$

reflects the loss of anion binding properties within the core of the permeation pathway, which contributes to the tight binding of SCN (Smith et al. 1999).

It is interesting that the charge-destroying mutation, R352A, had minimal effects on relative permeabilities but very significant effects on relative conductances. This might indicate that the consequences of mutations at R352 are felt more strongly deep within the pore, where the conformation of the narrow region establishes conductance rates, than at the wide cytoplasmic end of the pore, where R352 itself is predicted to lie. Indeed, our previous experiments (McCarty and Zhang 2001) showed that for small anions such as SCN^-, Br^- and NO_3^- relative conductance values are considerably more sensitive to the effects of pore-domain mutations than are relative permeability values. Our present results suggest

that loss of positive charge at position 352 destroyed the overall pore architecture, which subsequently changed the anion selectivity characteristics as seen in R352A- and R352E-CFTR. Therefore, it can be concluded that the preservation of positive charge at position 352 is very important for the maintenance of pore architecture of CFTR and the characteristics of anion selectivity. Furthermore, the finding that relative permeability values are nearly identical in R352A-, R352E- and R352K-CFTR suggests that the role of this site in determining anion selectivity is only indirect.

Mutations R352A and R347A Abolished Time-Dependent Block by Glipizide

Glipizide is a CFTR pore blocker from the sulfonylurea family of compounds which includes glibenclamide (Sheppard and Welsh 1992; Schultz et al. 1996; Sheppard and Robinson 1997; Zhang et al. 2004a, b). These compounds block WT-CFTR in a concentration-, voltage- and time-dependent manner; in previous experiments using a protocol identical to that used here, we showed that the apparent K_D for inhibition of WT-CFTR by glibenclamide at $V_M = -120$ mV was 27 μM (Zhang et al. 2004a). Glibenclamide and glipizide block the WT-CFTR pore at hyperpolarizing potentials by interacting with three binding sites: Equilibration with the first two is rapid, causing time-independent block, while equilibration with the third is slow, leading to time-dependent block (Zhang et al. 2004a, b). We hypothesized that a gross alteration of pore structure as a consequence of charge-neutralizing mutations at R352 would greatly affect block of the channel pore by glipizide.

Both R347A- and R352A-CFTR showed significantly weakened block by 200 μM glipizide, largely due to loss of the time-dependent component (Fig. 6). The average fractional block of WT-CFTR by 200 μM glipizide at $V_M = -120$ mV (0.48 ± 0.02, $n = 6$) was significantly different from the block of R352A-CFTR (0.33 ± 0.03, $n = 5$, $P = 0.004$). Similar results were found for block of R347A-CFTR (fractional block was 0.11 ± 0.02, $n = 5$, $P < 0.001$ compared to WT-CFTR). The gross change in pore architecture induced by both the R347A and R352A mutations appeared to have altered the kinetics of interaction with the site underlying slow block by glipizide, resulting in the loss of time-dependent inhibition. In contrast, the average fractional block of R352K-CFTR by 200 μM glipizide was not significantly different from the block of WT-CFTR at this concentration (0.52 ± 0.02, $n = 6$, $P = 0.119$) (Fig. 6G). Figure 6B, D, F, H shows the macroscopic *i–V* relationships for WT-, R352A-, R347A- and R352K-CFTR in representative experiments, indicating that glipizide blocked the currents primarily at negative membrane potentials in WT- and R352K-CFTR. However,

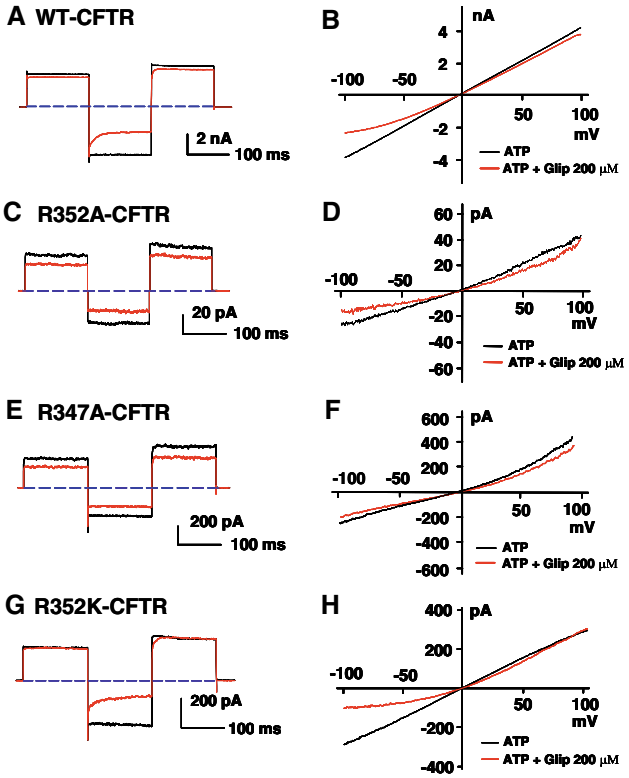

Fig. 6 Mutations at R352 alter pore pharmacology. *Left* Block of CFTR macropatch currents by glipizide (glip) was time-dependent in WT-CFTR (**A**) and R352K-CFTR (**G**) but not in R352A-CFTR (**C**) or R347A-CFTR (**E**). Each panel shows current in the absence (*black*) and in the presence of 200 μM glipizide (*red*), during voltage step protocols as described in "Methods." *Dashed line* indicates zero current level. *Right i–V* relationships for WT-CFTR (**B**), R352A-CFTR (**D**), R347A-CFTR (**F**) and R352K-CFTR (**H**) were constructed from voltage ramps performed in the absence (*black*) and in the presence of 200 μM glipizide (*red*). Solutions contained symmetrical ~150 mM [Cl^-], pH 7.5

the voltage dependence of block was clearly altered in R352A- and R347A-CFTR. Finally, R352A- and R347A-CFTR, but not R352K-CFTR, exhibited outward rectification of macroscopic currents in the absence of blocker, consistent with the outward rectification of single-channel amplitudes (Fig. 4, Table 1) (Cotten and Welsh 1999).

In summary, mutations at R352 that destroyed the positive charge (R352A, R352E and R352Q) altered the pore architecture of CFTR and caused instability of the open state, changing anion selectivity and pore block by glipizide. R352K-CFTR, in contrast, maintained the positive charge and most characteristics of WT-CFTR. This strongly suggests that R352 may serve a critical role in preserving the gross structure of the channel pore, perhaps by contributing to an interfacial pair with a negatively charged amino acid at another position in CFTR. To identify the acidic residue(s) that may interact with R352, we designed the following experiments.

D993 in TM9 Interacts with R352 in TM6

We hypothesized that R352 may mediate a stabilizing influence by contributing to an electrostatic interaction such as a salt bridge or hydrogen bonding pair within the MSDs (Creighton 1993; Glaser et al. 2001); salt bridges are important structural features that confer thermostability and resistance to denaturation to proteins (Perutz 1978). The distance between two residues in a salt bridge is typically 1.8–6.0 Å (average 3.5 Å) (Sharp and Honig 1990), making it likely that the potential partner of R352 would be localized within the MSDs. A computational study of protein–protein interfaces in 621 proteins indicated that arginine exhibits a strong preference for interaction with glutamic or aspartic acid (as well as tryptophan) (Glaser et al. 2001). Multiple glutamic acid and aspartic acid residues within the MSDs are likely within reach of R352: E92 (TM1), E873 (TM7), D924 (TM8), D993 (TM9) and E1104 (TM11). D924 already is known to form a salt bridge with R347 (Cotten and Welsh 1999). To identify the interaction partner for R352, we replaced R352 with an acidic residue (R352E) and introduced an arginine residue in the place of candidate interaction partners. We studied the conductance properties of CFTR channels bearing the following mutations: R352E, R352E/E873R, R352E/D993R and R352E/E1104R. Figure 7 shows representative currents (left) and all-points amplitude histograms (right) for these mutant channels under the same conditions as in Fig. 1. Three of these mutants, R352E-, R352E/E873R- and R352E/E1104R-CFTR, exhibited instability of the open state, in which the amplitudes of the *s1, s2* and *f* conductance states were very similar between the three mutants. R352E/D993R-CFTR, in contrast, exhibited stability of the full conductance state similar to that seen in WT-CFTR and R352K-CFTR (Fig. 1); transitions to the *s1* and *s2* states were rare events in this double mutant. Figure 8A shows the *i–V* relationship for the *f* conductance state for all four mutants, and WT-CFTR. R352E-, R352E/E873R- and R352E/E1104R-CFTR exhibited significant outward rectification, while WT-CFTR did not (Table 1). The slope conductance of R352E/D993R-CFTR was slightly lower than that of WT-CFTR, although linearity of the *i–V* relation was mostly retained. These data suggested that the D993R mutation at least partly compensated for the R352E mutation, although the double mutant R352E/D993R-CFTR did not fully recapitulate the behavior of WT-CFTR.

As discussed above, block of R352A-CFTR by glipizide was different from that of WT-CFTR in that the time-dependent component of block was lost (Fig. 6). If D993 served as the interaction partner of R352, we would expect that block of R352E/D993R-CFTR would be similar to that

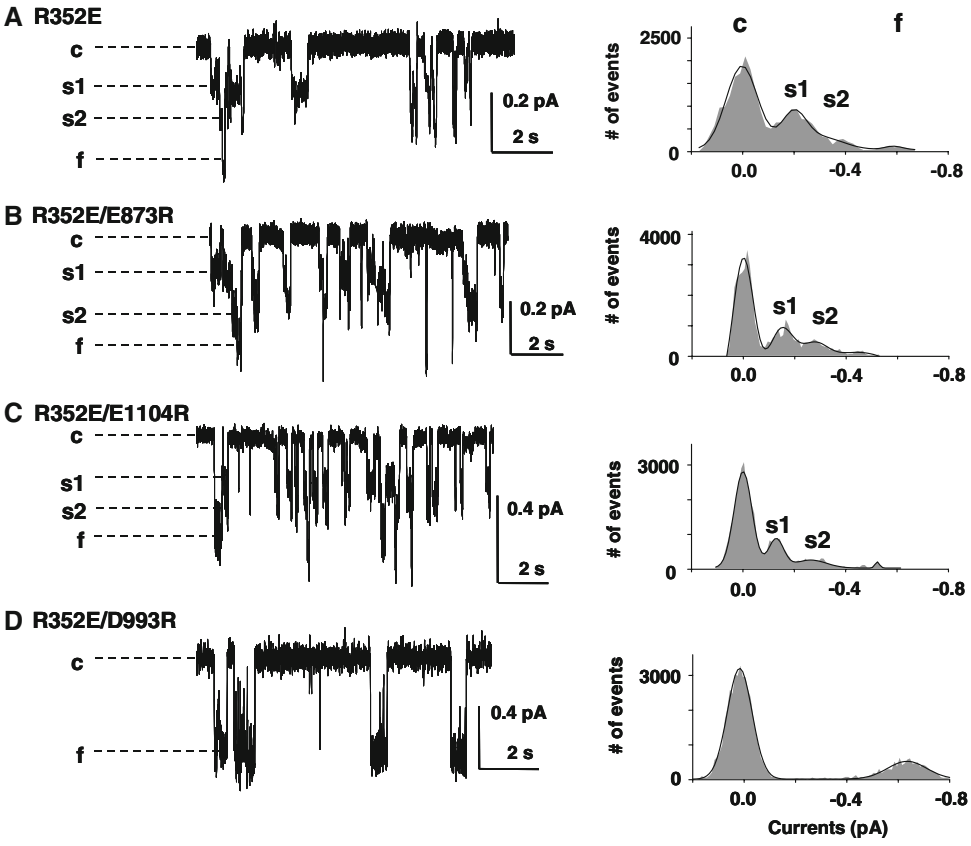

Fig. 7 Single-channel current tracings of R352E-CFTR and double mutants from excised inside–out patches (*left*) and resulting all-points amplitude histograms (*right*) under the same experimental conditions as in Fig. 1. Different conductance levels are indicated with *dashed lines*. There are four current levels indicating the *c, s1, s2* and *f* states in all but the revertant mutant R352E/D993R-CFTR, which only exhibited the *c* and *f* states. *Solid lines* in the panels at *right* are fit results to a gaussian function in Clampfit 9.0. All traces were recorded at $V_M = -100$ mV

seen for WT-CFTR. Figure 8B shows macropatch currents from R352E/D993R-CFTR in the presence and absence of 200 μM glipizide; time-dependent block was rescued in this double mutant. The average magnitude of fractional block by 200 μM glipizide at $V_M = -120$ mV (0.23 ± 0.05, $n = 5$), however, was significantly different from the block of WT-CFTR (0.48 ± 0.02, $n = 6$, $P < 0.001$). This result suggested that the revertant double mutation, R352E/D993R, recovered the time-dependent block by glipizide but did not completely recover the sensitivity to glipizide characteristic of WT-CFTR. This may reflect the difference in side chain volumes between aspartic and glutamic acids; the volume of a glutamic acid side chain is 20% larger than that of an aspartic acid side chain (Creighton 1993), which may result in a different pore structure.

To further explore the characteristics of R352E/D993R-CFTR, we studied anion selectivity between Cl^- and four substitute monovalent anions. Figure 5E shows a representative experiment in an excised inside–out macropatch under the same conditions as before. Overall, both relative permeability and relative conductance values for WT- and R352E/D993R-CFTR were similar (Tables 2, 3). R352E/D993R-CFTR currents exhibited the same anion permeability sequence as WT-CFTR: $SCN^- > NO_3^- \geq Br^- > Cl^-$ (although P_{SCN}/P_{Cl} was clearly reduced in the double mutant). R352E/D993R-CFTR exhibited relative conductances to SCN^- and Br^- intermediate between that of WT-CFTR and R352A-CFTR (Table 3). These results also suggested that R352A-CFTR and R352E/D993R-CFTR have different pore architecture and that the selectivity properties of the pore of the double mutant might be slightly different from that of WT-CFTR.

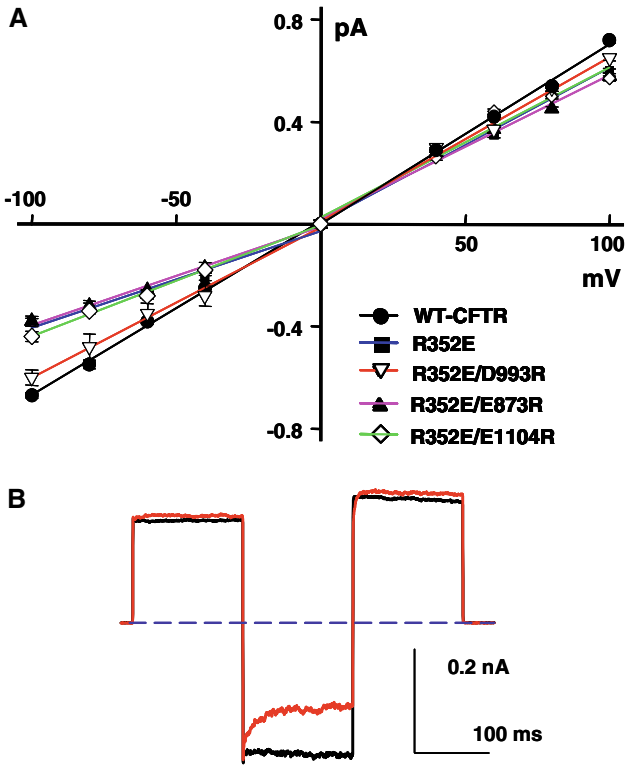

Fig. 8 The double mutant R352E/D993R-CFTR recovers WT-like channel behavior. (**A**) Single channel *i–V* relationships are shown for full conductance states of WT-, R352E-, R352E/E873R-, R352E/E1104R- and R352E/D993R-CFTR. Points show mean ± SEM for $n = 5$–7 observations each, and many error bars are smaller than the symbols; *lines* are from linear regression. (**B**) Block of R352E/D993R-CFTR macropatch currents by glipizide (200 μM) is time-dependent. Experimental conditions are the same as in Fig. 6. *Red line* indicates current in the presence of glipizide; *dashed line* is zero-current level. Fractional block was measured at the end of the pulse to $V_M = -120$ mV

The D993R Mutation Alone also Altered the Pore Architecture of CFTR

D993 is localized to TM9 of CFTR, which has not been suggested to be a pore lining domain (McCarty 2000). Because the data presented thus far suggested that D993 serves as the interacting partner of R352, we predicted that the D993R mutation alone would change channel activity in a manner similar to that of the R352E, -A or -Q mutation. We studied D993R-CFTR with single-channel recording techniques using the same conditions as in Fig. 1. D993R-CFTR exhibited instability of the open state, with frequent transitions between all three open conductance levels (Fig. 9A, B); these three open states were even less stable than those of R352A-CFTR. The slope conductance of the *f* state in D993R-CFTR was larger than that of WT-CFTR and indicated slight inward rectification (Fig. 9C, Table 1). These results suggest that the D993R mutation alone also destroyed pore architecture in a manner similar to that of the charge-destroying mutations at R352.

Disruption of Pore Architecture Alters Reactivity of Endogenous Cysteine(s)

As a final test of our hypothesis that charge-altering mutations at R352 alter the gross structure of the channel pore, we asked whether such mutations impacted the sensitivity to chemical modification by externally applied thiol reagents. We previously reported that a cysteine engineered at R352 either was not accessible to the membrane-impermeable reagents $MTSES^-$ and $MTSET^+$ applied externally or lacked significant functional consequences when modified, although R352C-CFTR (but not WT-CFTR) did respond to prolonged exposure to the membrane-permeant $MTSEA^+$ (Smith et al. 2001). Surprisingly, similar results were found in R352Q-CFTR, suggesting that the response to $MTSEA^+$ in R352C-CFTR was nonspecific, not being due to modification of that engineered cysteine. WT-CFTR bears 18 endogenous cysteines. Hence, it is likely that $MTSEA^+$ modified one (or more) of the endogenous cysteines, which

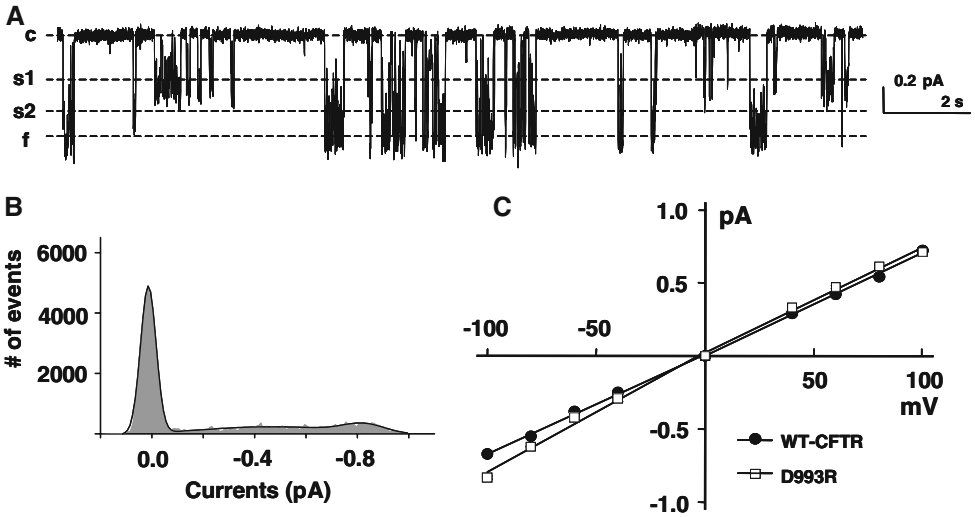

Fig. 9 Mutation D993R alone had effects similar to those of the charge-reversing mutations at R352. Representative single-channel current tracing (**A**), all-points amplitude histogram (**B**) and *i–V* relationship for the *f* conductance state (**C**) are shown for the D993R mutant. Currents were obtained under the same conditions as in the experiment shown in Fig. 1, $V_M = -100$ mV. In **c**, points show mean ± SEM for $n = 7$ observations, and error bars are smaller than the symbols; *lines* are from linear regression

became available for covalent modification due to the loss of protein structure resulting from destruction of the salt bridge at R352. If this were true, we would expect that the revertant double mutant, R352E/D993R-CFTR, would not respond to $MTSEA^+$. We tested this hypothesis using two-electrode voltage-clamp measurements of CFTR currents activated by isoproterenol in oocytes expressing CFTR and the human β_2-adrenergic receptor. After isoproterenol-activated currents reached steady state, cells were exposed to 1 mM $MTSEA^+$ in the continuous presence of isoproterenol. $MTSEA^+$ led to a transient increase in WT-CFTR current but a sustained increase in R352A-CFTR current (Fig. 10). After 5 min of incubation, WT-CFTR exhibited a 1.11 ± 0.05-fold increase, while R352A-CFTR exhibited a 1.30 ± 0.07-fold increase ($n = 3$ each, $P = 0.021$). In contrast, R352E/D993R-CFTR was insensitive to exposure to $MTSEA^+$, which resulted in only a 1.08 ± 0.02-fold increase in current ($n = 6$), thus indicating that the double mutant exhibited WT-like behavior.

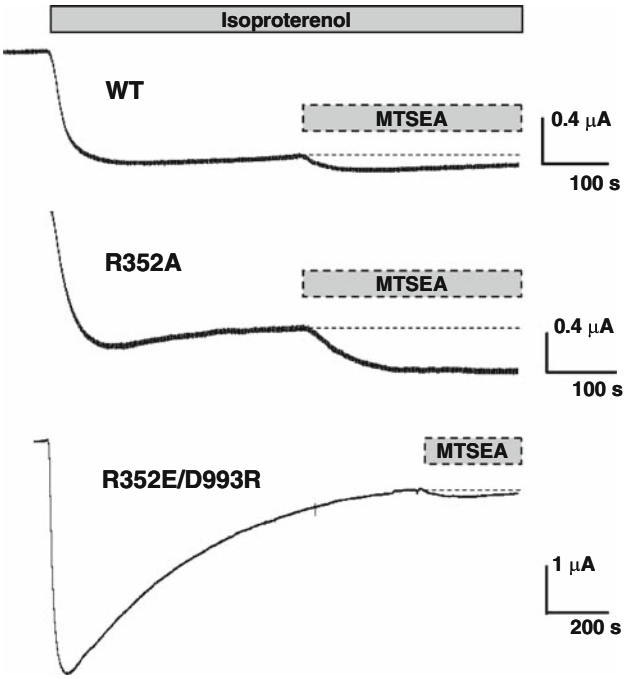

Fig. 10 Mutation R352A results in appearance of sensitivity to a cysteine-modifying reagent. Oocytes expressing WT-CFTR (*top trace*), R352A-CFTR (*middle trace*) or R352E/D993R-CFTR (*bottom trace*), along with the β_2-adrenergic receptor, were studied by two-electrode voltage clamp. CFTR currents were activated by exposure to isoproterenol (1 μM). After currents reached steady state, cells were exposed to 1 mM $MTSEA^+$ for 5 min in the continuing presence of isoproterenol. Holding potential = −60 mV

Discussion

R352 Stabilizes the Open State in WT-CFTR

The results presented here are compatible with the hypothesis that R352 in TM6 of CFTR functions at least in part by contributing to an interaction with D993 in TM9, perhaps by forming a salt bridge. First, channels bearing charge-destroying mutations at this site, including R352Q, R352E and R352A, exhibited instability of the open state compared to WT-CFTR, as indicated by frequent transitions between all three open conductance states (*s1, s2, f*). These mutant CFTRs also exhibited anion selectivity patterns different from that of WT-CFTR, and time-dependent block by glipizide was lost. In contrast, channels bearing the charge-conserving mutation R352K showed characteristics similar to WT-CFTR. R352A-CFTR exhibited outward rectification in conditions of symmetrical [Cl^-], similar to that found in R347A-CFTR (Fig. 6). These results strongly suggested that the loss of the positively charged side chain at position 352 shifted the pore architecture in such a way as to destabilize the full open state,

likely due to the involvement of R352 in forming a stabilizing interaction with an acidic residue. Second, we identified the interaction partner as D993 by use of double mutants; R352E/E873R-CFTR and R352E/E1104R-CFTR exhibited permeation properties similar to those of R352E-CFTR, while R352E/D993R-CFTR behaved more like WT-CFTR. In this charge-swapping double mutant, the *f* conductance state was the dominant open state while states *s1* and *s2* were rare, time-dependent block by glipizide was recovered, and anion selectivity patterns were similar to those of WT-CFTR. Third, we showed that the interaction between R352 and D993 also could be disrupted by a charge reversal mutation at D993. As predicted, D993R-CFTR exhibited instability of the open state similar to that seen in R352E-CFTR.

Previous work suggested that residues at the cytoplasmic end of TM6 (including T351, R352 and Q353) might form a reentrant loop directed back into the channel pore, narrowing the lumen and thereby forming both the charge selectivity filter and the major resistance to current flow (Cheung and Akabas 1997; Guinamard and Akabas 1999). Designation of R352 as the anion selectivity filter was predominantly based upon differences in the rates of modification of engineered cysteines at this site (in R352C-CFTR) by positively and negatively charged sulfhydryl modifying reagents, $MTSET^+$ and $MTSES^-$ (Cheung and Akabas 1997; Guinamard and Akabas 1999). However, control experiments were not included in that study in order to ensure that the results could be attributed to the single engineered cysteine. Also, near the predicted cytoplasmic end of the CFTR pore, substitutions of the arginine at position 347 by any residue other than lysine destabilized the pore structure, while the double mutation R347D/D924R recovered open state stability, suggesting that R347 formed a salt bridge with D924 in the wild-type channel (Cotten and Welsh 1999). Hence, R347 plays an important structural role in CFTR, and many of the functions previously ascribed to this site, including anion binding (Tabcharani et al. 1993), control of susceptibility to block by cytoplasmic DIDS (Linsdell and Hanrahan 1996a, b), control of iodide permeability (Tabcharani et al. 1997) and determination of anion/cation selectivity (Cheung and Akabas 1997), most likely were only indirectly affected by charge-destroying mutations at this site. Mutations at R347 also inhibited ATPase activity at the NBDs (Ramjeesingh et al. 2001), suggesting that loss of the salt bridge involving this residue has profound effects on protein structure and function that may be propagated to a great distance within the folded polypeptide.

Our results are not consistent with the notion that R352 simply provides a positive surface charge at the intracellular end of the pore, as proposed by St. Aubin and Linsdell (2006). In that study, the authors examined the effects of mutations at R352 and at R303, the latter of which is thought to contribute to the intracellular end of TM5. Glutamine and glutamic acid substitutions at these positions induced outward rectification in the presence of symmetrical [Cl^-] and reduced single-channel conductance. However, the changes in both of these parameters upon introduction of negative charge (i.e., glutamic acid compared to glutamine) were much larger for mutations at R303 than at R352. This suggests that R303 and R352 may serve different structural roles in the WT channel.

Contributions of R352 to Pore Architecture

We recently showed that a single anion-conducting pore is formed by a single CFTR polypeptide (Zhang et al. 2005a). However, other authors reported that the amino-terminal portion of CFTR, containing MSD1, NBD1 and the R domain (D836X-CFTR), formed regulated Cl^- channels that differed somewhat from WT-CFTR (Sheppard et al. 1994). Although the substate behavior of D836X-CFTR was not studied in detail, this mutant was reported to show instability of the open state compared to WT-CFTR; the authors suggested that residues in MSD2 might stabilize the channel complex, perhaps assisting in the arrangement of residues in MSD1 into a functional structure, based on the finding that the number of functional Cl^- channels generated from the D836X construct was much lower than expected for WT-CFTR. Other authors also reported that constructs encoding only the amino-terminal (front) half (Yue et al. 2000) or only the carboxy-terminal (back) half (Ramjeesingh et al. 2003) of CFTR can form functional channels when expressed individually, although it is very likely that two front-half CFTRs or two back-half CFTRs form homodimers to create functional channels (Zhang et al. 2005a). Biochemical experiments also indicated that integration of peptides comprising only MSD1 of CFTR into lipid bilayers was extremely unstable (Tector and Hartl 1999). These findings suggest that two MSDs must function together to form a stable chloride channel.

In the WT-CFTR channel, the interaction partner of R347 (D924) is in TM8 (Cotten and Welsh 1999) and the interaction partner of R352 (D993) is in TM9 (present work). Hence, two sites in MSD1 have now been linked to sites in MSD2, making it clear that both halves of the full CFTR polypeptide are required for formation of the functional channel. Several R352 mutations are CF-associated mutations, including R352G, R352W and R352Q (Cremonesi et al. 1992; Audrézet et al. 1993; Brancolini et al. 1995; Feldmann et al. 2003); similarly, D993Y and D993G are associated with disease (Tsui et al. 2007). Our data suggest that CF-associated mutations, as well as other charge-destroying mutations, at these sites affect CFTR

function similarly in that they alter pore structure by disrupting the interaction between R352 and D993. These data highlight the importance of R352 for CFTR function and may explain in part why this residue is the locus of multiple CF-associated mutations. Consistent with the important structural role for R352 and D993 in stabilizing the channel's tertiary structure, which we propose here, Chen et al. (2001) showed that both of these sites are conserved across CFTR sequences from mammalian and nonmammalian species ranging from dogfish to human.

Disruption of the R352/D993 Interaction May Affect Channel Gating

Salt bridges are key structural elements in channels, and their disruption can affect properties of both permeation and gating. Arginine and lysine residues through electrostatic interactions with anionic residues are important for the structure of membrane-spanning domains in many other proteins, such as Lac permease and the inwardly rectifying K^+ channel (IRK1) (King et al. 1991; Yang et al. 1997). Disrupting the E145/R155 salt bridge in Kir3.4 abolished selectivity for K^+ and agonist activation of these channels (Claydon et al. 2003). The role of salt bridges in channel gating was also studied in HCN2 and CNGA1 channels. The K472E mutant of HCN2 was activated slowly and no longer modulated by cAMP; the R431E mutant of CNGA1 exhibited an increase in the favorability of channel opening. The WT behavior of both HCN2 and CNGA1 channels was rescued by swapping the positions of the basic and acidic interacting residues, thus restoring the salt bridges (Craven and Zagotta 2004). Finally, porins are trimeric channel-forming proteins of the outer membrane of *Escherichia coli*. Disruptions of salt bridges between residues D118, R174 and R92 of the L3 loop in OmpC porin affected gating by increasing the activity of spontaneous transitions (Liu and Delacour 1998). In other ABC transporters, salt bridges have been identified within the NBDs (Zaitseva et al. 2006; Kitaoka et al. 2006) and periplasmic binding proteins (Stockner et al. 2005; Abbott and Boraston 2007) and between a periplasmic binding protein and its cognate TM domain (Braun and Herrmann 2007), but salt bridges within the TM domains have not been described to date, except in CFTR (Cotten and Welsh 1999).

Our data show that instability of the open state could be induced by charge-destroying mutations at either R352 or D993. Stability of the open state was retained in the case of a charge-conserving mutation, R352K, and in the double mutant R352E/D993R-CFTR. However, a major difference between our work with R352 and the previous work with R347 (Cotten and Welsh 1999) is that we showed that repairing the salt bridge in the double mutant does not fully recapitulate the permeation properties of WT-CFTR. Compared to WT-CFTR, R352E/D993R-CFTR channels exhibited lower slope conductance, weakened block by glipizide, and altered selectivity between Cl^- and SCN^-. The fact that differences in anion selectivity remain between R352K- and WT-CFTR is consistent with the notion that interactions between lysine and the aspartic acid at D993 are not the same as the interactions between arginine and D993. We consider it likely that this difference in side-chain volume and/or orientation results in distortions of the pore structure, including in the narrow portion of the pore where selectivity between ions is strongest, and that this results in the observed differences in relative conductances. We also note that while the relative conductance values for SCN^-, Br^- and NO_3^- are shifted in the same direction in R352K-CFTR as they are in R352A- or R352E-CFTR, the shifts for SCN^- and Br^- are smaller in R352K-CFTR than in the charge-destroying mutants. We conclude that the double mutant R352E/D993R-CFTR retains the interaction between these residues but does not fully mimic the behavior of WT-CFTR, suggesting that permeation properties in the CFTR chloride channel are very sensitive to small changes in pore structure.

CFTR is a member of the ABC transporter superfamily and is regulated by PKA-mediated phosphorylation plus ATP hydrolysis at NBD1 and NBD2. However, the mechanism by which the binding and hydrolysis of ATP at the NBDs is coupled to gating the permeation pathway is not known. The functional conducting states that can be visited by the protein, with their associated rates of permeation, may depend on small and local structural rearrangements within the pore brought about as a consequence of ATP-dependent gating. The stability of the open state(s) and the consistency of biophysical properties of permeation likely rely upon a stable architecture of the membrane-spanning domains in the folded polypeptide. We predict that disruption of the interaction between R352 and D993 alters the architecture of the CFTR pore, resulting in effects on both permeation and pore gating. Indeed, it seems likely that the interaction between these sites is formed during channel opening and then broken during the conformational changes underlying channel closure. These studies may provide a tool to probe the connection between conformational changes in the pore and the energy of hydrolysis of ATP.

Acknowledgements We thank Chris Thompson for comments. This work was supported by the National Institute for Diabetes, Digestive and Kidney Diseases (DK056481 to N. A. M.) and the Cystic Fibrosis Foundation (MCCART07P0). During the performance of these studies, N. A. M. was an Established Investigator of the American Heart Association.

References

Abbott DW, Boraston AB (2007) Specific recognition of saturated and 4,5-unsaturated hexuronate sugars by a periplasmic binding protein involved in pectin catabolism. J Mol Biol 369:759–770

Anderson MP, Gregory RJ, Thompson S, Souza DW, Paul S, Mulligan RC, Smith AE, Welsh MJ (1991) Demonstration that CFTR is a chloride channel by alteration of its anion selectivity. Science 253:202–205

Audrézet M-P, Mercier B, Guillermit H, Quere I, Verlingue C, Rault G, Ferec C (1993) Identification of 12 novel mutations in the CFTR gene. Hum Mol Genet 2:51–54

Baukrowitz T, Hwang T-C, Nairn AC, Gadsby DC (1994) Coupling of CFTR Cl^- channel gating to an ATP hydrolysis cycle. Neuron 12:473–482

Brancolini V, Cremonesi L, Belloni E, Pappalardo E, Bordoni R, Seia M, Rady M, Russo MP, Romeo G, Devoto M (1995) Search for mutations in pancreatic sufficient cystic fibrosis Italian patients: detection of 90% of molecular defects and identification of three novel mutations. Hum Genet 96:312–318

Braun V, Herrmann C (2007) Docking of the periplasmic FecB binding protein to the FecCD transmembrane proteins in the ferric citrate transport system of *Escherichia coli*. J Bacteriol 189:6913–6918

Chen JM, Cutler C, Jacques C, Boefu G, Denamur E, Lecointre G, Mercier B, Cramb G, Férec C (2001) A combined analysis of the cystic fibrosis transmembrane conductance regulator: implications for structure and disease models. Mol Biol Evol 18:1771–1788

Cheng SH, Gregory RJ, Marshall J, Paul S, Souza DW, White GA, O'Riordan CR, Smith AE (1990) Defective intracellular transport and processing of CFTR is the molecular basis of most cystic fibrosis. Cell 63:827–834

Cheng SH, Rich DP, Marshall J, Gregory RJ, Welsh MW, Smith AE (1991) Phosphorylation of the R domain by cAMP-dependent protein kinase regulates the CFTR chloride channel. Cell 66:1027–1036

Cheung M, Akabas MH (1997) Locating the anion-selectivity filter of the cystic fibrosis transmembrane conductance regulator (CFTR) chloride channel. J Gen Physiol 109:289–299

Claydon TW, Makary SY, Dibb KM, Boyett MR (2003) The selectivity filter may act as the agonist-activated gate in the G protein-activated Kir3.1/Kir3.4 K^+ channel. J Biol Chem 278:50654–50663

Cotten JF, Welsh MJ (1999) Cystic fibrosis-associated mutations at arginine 347 alter the pore architecture for CFTR: evidence for disruption of a salt bridge. J Biol Chem 274:5429–5435

Craven KB, Zagotta WN (2004) Salt bridges and gating in the COOH-terminal region of HCN2 and CNGA1 channels. J Gen Physiol 124:663–677

Creighton TE (1993) Proteins: structure and molecular properties. WH Freeman, New York

Cremonesi L, Ferrari M, Belloni E, Magnani C, Seia M, Ronchetto P, Rady M, Russo MP, Romeo G, Devoto M (1992) Four new mutations of the CFTR gene (541delC, R347H, R352Q, E585X) detected by DGGE analysis in Italian CF patients, associated with different clinical phenotypes. Hum Mutat 1:314–319

Dean M, Homon Y, Chimini G (2001) The human ATP-binding cassette (ABC) transporter superfamily. J Lipid Res 42:1007–1017

Devidas S, Guggino WB (1997) CFTR: domains, structure, and function. J Bioenerg Biomemb 29:443–451

Feldmann D, Couderc R, Audrézet M-P, Ferec C, Bienvenu T, Desgeorges M, Claustres M, Mittre H, Blayau M, Bozon D, Malinge MC, Monnier M, Bonnefont JP, Iron A, Bieth E, Dumur V, Clavel C, Cazeneuve C, Girodon E (2003) CFTR genotypes in patients with normal or borderline sweat chloride levels. Hum Mutat 22:340

Gadsby DC, Vergani P, Csanády L (2006) The ABC protein turned chloride channel whose failure causes cystic fibrosis. Nature 440:477–483

Ge N, Muise C, Gong X, Linsdell P (2004) Direct comparison of the functional roles played by different transmembrane regions in the cystic fibrosis transmembrane conductance regulator chloride channel pore. J Biol Chem 279:55283–55289

Glaser F, Steinberg DM, Vakser IA, Ben-Tal N (2001) Residue frequencies and pairing preferences at protein–protein interfaces. Proteins 43:89–102

Guggino WB, Stanton BA (2006) New insights into cystic fibrosis: molecular switches that regulate CFTR. Nat Rev Mol Cell Biol 7:426–436

Guinamard R, Akabas MH (1999) Arg352 is a major determinant of charge selectivity in the cystic fibrosis transmembrane conductance regulator chloride channel. Biochemistry 38:5528–5537

Hwang T-C, Nagel G, Nairn AC, Gadsby DC (1994) Regulation of the gating of cystic fibrosis transmembrane conductance regulator Cl channels by phosphorylation and ATP hydrolysis. Proc Natl Acad Sci USA 91:4698–4702

King SC, Hansen CL, Wilson TH (1991) The interaction between aspartic acid 237 and lysine 358 in the lactose carrier of *Escherichia coli*. Biochim Biophys Acta 1062:177–186

Kitaoka S, Wada K, Hasegawa Y, Minami Y, Fukuyama K, Takahashi Y (2006) Crystal structure of *Escherichia coli* SufC, an ABC-type ATPase component of the SUF iron–sulfur cluster assembly machinery. FEBS Lett 580:137–143

Linsdell P (2001) Thiocyanate as a probe of the cystic fibrosis transmembrane conductance regulator chloride channel pore. Can J Physiol Pharmacol 79:573–579

Linsdell P (2005) Location of a common inhibitor binding site in the cytoplasmic vestibule of the cystic fibrosis transmembrane conductance regulator chloride channel pore. J Biol Chem 280:8945–8950

Linsdell P (2006) Mechanism of chloride permeation in the cystic fibrosis transmembrane conductance regulator chloride channel. Exp Physiol 91:123–129

Linsdell P, Hanrahan JW (1996a) Disulphonic stilbene block of cystic fibrosis transmembrane conductance regulator Cl^- channels expressed in a mammalian cell line, and its regulation by a critical pore residue. J Physiol 496:687–693

Linsdell P, Hanrahan JW (1996b) Flickery block of single CFTR chloride channels by intracellular anions and osmolytes. Am J Physiol 271:C628–C634

Linsdell P, Tabcharani JA, Rommens JM, Hou Y-X, Chang X-B, Tsui L-C, Riordan JR, Hanrahan JW (1997) Permeability of wild-type and mutant cystic fibrosis transmembrane conductance regulator chloride channels to polyatomic anions. J Gen Physiol 110:355–364

Linsdell P, Evagelidis A, Hanrahan JW (2000) Molecular determinants of anion selectivity in the cystic fibrosis transmembrane conductance regulator chloride channel pore. Biophys J 78:2973–2982

Liu NZ, Delcour AH (1998) The spontaneous gating activity of OmpC porin is affected by mutations of a putative hydrogen bond network or of a salt bridge between the L3 loop and the barrel. Protein Eng 11:797–802

Liu X, Zhang Z-R, Fuller MD, Billingsley J, McCarty NA, Dawson DC (2004) CFTR: a cysteine at position 338 in TM6 senses a positive electrostatic potential in the pore. Biophys J 87:3826–3841

McCarty NA (2000) Permeation through the CFTR chloride channel. J Exp Biol 203:1947–1962

McCarty NA, Zhang Z-R (2001) Identification of a region of strong discrimination in the pore of CFTR. Am J Physiol 281:L852–L867

McDonough S, Davidson N, Lester HA, McCarty NA (1994) Novel pore-lining residues in CFTR that govern permeation and open-channel block. Neuron 13:623–634

Perutz MF (1978) Electrostatic effects in proteins. Science 201:1187–1191

Qin F, Auerbach A, Sachs F (1996) Estimating single-channel kinetic parameters from idealized patch clamp data containing missed events. Biophys J 70:264–280

Ramjeesingh M, Li C, Kogan I, Wang Y, Huan L-J, Bear CE (2001) A monomer is the minimum function unit required for channel and ATPase activity of the cystic fibrosis transmembrane conductance regulator. Biochemistry 40:10700–10706

Ramjeesingh M, Ugwu F, Li C, Dhani S, Huan L-J, Wang Y, Bear CE (2003) Stable dimeric assembly of the second membrane-spanning domain of CFTR (cystic fibrosis transmembrane conductance regulator) reconstitutes a chloride-selective pore. Biochemistry 375:633–641

Riordan JR, Rommens JM, Kerem B-S, Alon N, Rozmahel R, Grzelczak Z, Zielenski J, Lok S, Plavsic N, Chou J-L, Drumm ML, Iannuzzi MC, Collins FS, Tsui L-C (1989) Identification of the cystic fibrosis gene: cloning and characterization of complementary DNA. Science 245:1066–1072

Schultz BD, DeRoos ADG, Venglarik CJ, Singh AK, Frizzell RA, Bridges RJ (1996) Glibenclamide blockade of CFTR chloride channels. Am J Physiol 271:L192–L200

Sharp KA, Honig B (1990) Electrostatic interactions in macromolecules: theory and applications. Annu Rev Biophys Biophys Chem 19:301–332

Sheppard DN, Robinson KA (1997) Mechanism of glibenclamide inhibition of cystic fibrosis transmembrane conductance regulator Cl^- channels expressed in a murine cell line. J Physiol 503:333–345

Sheppard DN, Welsh MJ (1992) Effect of ATP-sensitive K^+ channel regulators on cystic fibrosis transmembrane conductance regulator chloride currents. J Gen Physiol 100:573–592

Sheppard DN, Ostedgaard LS, Rich DP, Welsh MJ (1994) The amino-terminal portion of CFTR forms a regulated Cl^- channel. Cell 76:1091–1098

Sheppard DN, Travis SM, Ishihara H, Welsh MJ (1996) Contributions of proline residues in the membrane-spanning domains of the cystic fibrosis transmembrane conductance regulator to chloride channel function. J Biol Chem 271:14995–15001

Smith SS, Steinle ED, Meyerhoff ME, Dawson DC (1999) Cystic fibrosis transmembrane conductance regulator: physical basis for lyotropic anion selectivity patterns. J Gen Physiol 114:799–817

Smith SS, Liu X, Zhan Z-R, Sun F, Kriewall TE, McCarty NA, Dawson DC (2001) CFTR: covalent and noncovalent modification suggests a role for fixed charges in anion conduction. J Gen Physiol 118:407–431

St. Aubin CN, Linsdell P (2006) Positive charges at the intracellular mouth of the pore regulate anion conduction in the CFTR chloride channel. J Gen Physiol 128:535–545

Stockner T, Vogel HJ, Tieleman DP (2005) A salt-bridge motif involved in ligand binding and large-scale domain motions of the maltose-binding protein. Biophys J 89:3362–3371

Tabcharani JA, Rommens JM, Hou Y-X, Chang X-B, Tsui L-C, Riordan JR, Hanrahan JW (1993) Multi-ion pore behavior in the CFTR chloride channel. Nature 366:79–82

Tabcharani JA, Linsdell P, Hanrahan JW (1997) Halide permeation in wild-type and mutant cystic fibrosis transmembrane conductance regulator chloride channels. J Gen Physiol 110:341–351

Tector M, Hartl FU (1999) An unstable transmembrane segment in the cystic fibrosis transmembrane conductance regulator. EMBO J 18:6290–6298

Tsui L-C, Zielenski J, O'Brien A (2007) Cystic Fibrosis Mutation Database, http://www.genet.sickkids.on.ca/cftr/Home.html

Yang J, Yu M, Jan YN, Jan LY (1997) Stabilization of ion selectivity filter by pore loop pairs in an inwardly rectifying potassium channel. Proc Natl Acad Sci USA 94:1568–1572

Yue H, Devidas S, Guggino WB (2000) The two halves of CFTR form a dual-pore ion channel. J Biol Chem 275:10030–10034

Zaitseva J, Oswald C, Jumpertz T, Jenewein S, Wiedenmann A, Holland IB, Schmitt L (2006) A structural analysis of asymmetry required for catalytic activity of an ABC-ATPase domain dimer. EMBO J 25:3432–3443

Zhang Z-R, McDonough SI, McCarty NA (2000) Interaction between permeation and gating in a putative pore-domain mutant in CFTR. Biophys J 79:298–313

Zhang Z-R, Zeltwanger S, Smith SS, Dawson DC, McCarty NA (2001) Voltage-sensitive gating induced by a mutation in the fifth transmembrane domain of CFTR. Am J Physiol 282:L135–L145

Zhang Z-R, Cui G, Zeltwanger S, McCarty NA (2004a) Time-dependent interactions of glibenclamide with CFTR: kinetically complex block of macroscopic currents. J Membr Biol 201:139–155

Zhang Z-R, Zeltwanger S, McCarty NA (2004b) Steady-state interactions of glibenclamide with CFTR: evidence for multiple sites. J Membr Biol 199:15–28

Zhang Z-R, Cui G, Liu X, Song B, Dawson DC, McCarty NA (2005a) Determination of the functional unit of the cystic fibrosis transmembrane conductance regulator chloride channel: one polypeptide forms one pore. J Biol Chem 280:458–468

Zhang Z-R, Song B, McCarty NA (2005b) State-dependent chemical reactivity of an engineered cysteine reveals conformational changes in the outer vestibule of CFTR. J Biol Chem 280:41997–42003